

# Noninvasive *in Situ* Evaluation of Osteogenic Differentiation by Time-Resolved Laser-Induced Fluorescence Spectroscopy

PETER ASHJIAN, M.D.,<sup>1</sup> AMIR ELBARBARY, M.D.,<sup>1</sup> PATRICIA ZUK, Ph.D.,<sup>1</sup>  
DANIEL A. DEUGARTE, M.D.,<sup>1</sup> PROSPER BENHAIM, M.D.,<sup>1</sup> LAURA MARCU, Ph.D.,<sup>2,3</sup>  
and MARC H. HEDRICK, M.D.<sup>1</sup>

## ABSTRACT

The clinical implantation of bioengineered tissues requires an *in situ* nondestructive evaluation of the quality of tissue constructs developed *in vitro* before transplantation. Time-resolved laser-induced fluorescence spectroscopy (TR-LIFS) is demonstrated here to noninvasively monitor the formation of osteogenic extracellular matrix (ECM) produced by putative stem cells (PLA cells) derived from human adipose tissue. We show that this optical spectroscopy technique can assess the relative expression of collagens (types I, III, IV, and V) within newly forming osteogenic ECM. The results are consistent with those obtained by conventional histochemical techniques (immunofluorescence and Western blot) and demonstrate that TR-LIFS is a potential tool for monitoring the expression of distinct collagen types and the formation of collagen cross-links in intact tissue constructs.

## INTRODUCTION

AS TISSUE ENGINEERING becomes a clinical reality, a novel means of evaluating tissue constructs before transplantation that are noninvasive, and nondestructive, become essential. These are important for tissue-engineering development and application because traditional methods of evaluation require fixation, serial sectioning, histology, and/or immunocytochemistry, methods that are inherently invasive and injurious. Although revealing information about the molecular changes taking place in bioengineered tissues, they are clinically restrictive because of construct damage, rendering them unsuitable for patient utilization. We report here a nondestructive, noninvasive methodology, and demonstrate that time-

solved (lifetime) laser-induced fluorescence spectroscopy (TR-LIFS) could provide such a critical and desirous technique. This optical methodology is demonstrated to monitor the evolution of osteogenic differentiation and thus is an important potential tool for the *in situ*, noninvasive, and nondestructive evaluation of bioengineered tissues.

Fluorescence spectroscopy has been successfully applied, both at research and clinical levels, to the detection of pathologic and physiological transformations of biological tissues (neoplasia, dermal lesions, and atherosclerotic plaques).<sup>1-8</sup> Tissue fluorescence originates from several endogenous fluorescent biomolecules (fluorophores) including structural proteins (elastin, collagen), amino acids (tryptophan, tyrosine, and phenylala-

<sup>1</sup>Laboratory for Regenerative Bioengineering and Repair, Departments of Surgery and Orthopedics, UCLA School of Medicine, Los Angeles, CA 90095.

<sup>2</sup>Biophotonics Research and Technology Development, Department of Surgery, MIST Institute, Cedars-Sinai Medical Center, Los Angeles, CA 90048.

<sup>3</sup>Departments of Biomedical and Electrical Engineering, University of Southern California, Los Angeles, CA 90089.

nine), porphyrins, and enzyme cofactors (NADH and FAD).<sup>1,2,6,9</sup> The fluorescence emission of these fluorophores has been investigated both *in vitro* and *in vivo*.<sup>1-10</sup> Pathologic, physiologic, and metabolic transformations result in associate modifications at the molecular level, including the deposition and/or alteration of native tissue fluorophores. The composite fluorescence pattern of a tissue reflects the relative contribution of individual fluorophores, thus fluorescence features can be correlated with the biochemical composition of the tissue and the associated pathological or physiological conditions. Time-resolved information improves the specificity of fluorescence measurements and currently is used for the diagnosis of cancer and staging of atherosclerotic plaques.<sup>4,11-13</sup>

As osteogenic tissue develops, the tissue undergoes an ordered series of events, namely osteoblast proliferation, matrix synthesis, maturation, and ultimately matrix mineralization.<sup>14</sup> The final stages of development are defined by the biosynthesis and organization of the bone extracellular matrix (ECM), containing predominantly collagen type I, with trace amounts of type III and V collagens depending on developmental stage.<sup>14-20</sup> Monitoring osteogenic differentiation at these stages is essential because bioengineered bone constructs must achieve functional maturity before implantation.

Conventional methods of assessing osteogenic differentiation include assaying for collagen type I content and/or the ratio of collagen I to other collagen subtypes. This is important for our study because the information about extracellular matrix protein expression inferred using conventional techniques of immunofluorescence (IF), immunohistochemistry, and Western blot analysis can be contrasted against a spectroscopic assessment of tissue collagen—which is one of the most fluorescent biomolecules in tissue.<sup>21-28</sup> The present study sought to determine the feasibility of TR-LIFS to determine the changes in collagen expression within an osteogenic matrix produced by a population of putative stem cells derived from human adipose tissue (termed processed lipoaspirate [PLA] cells<sup>29-31</sup>). The results of this work show the potential of TR-LIFS for noninvasively analyzing the quality of tissue-engineered bone constructs before patient implantation.

## MATERIALS AND METHODS

### *Osteogenic differentiation of human PLA cells*

All studies involving human subjects were approved by the University of California, Los Angeles (UCLA) Institutional Review Board (HSPC 98-08-011-04). Informed written consent was acquired from each patient before the procedure. PLA cells, derived from human lipoaspirates ( $n = 3$ ; ages, 34–39 years) were isolated and cultured in control medium (CM) (Table 1).<sup>29</sup> To induce osteogenesis, cells were grown to 70–80% confluency and cultured in osteogenic medium (OM) for 3, 5, and 7 weeks. To confirm osteogenesis, PLA samples were analyzed by histochemical staining for alkaline phosphatase (AP) activity and matrix calcification (von Kossa stain) as described elsewhere.<sup>29</sup> In addition, samples were analyzed by conventional reverse transcription-polymerase chain reaction (RT-PCR), using primer sets to the osteogenic genes encoding osteopontin, osteonectin, osteocalcin, CBFA-1, and alkaline phosphatase (Table 2).<sup>31</sup> Duplicate PCRs for  $\beta$ -actin were used as an internal control. A human osteoblast cell line (NH0st cells; Cambrex Bio Science Walkersville, Walkersville, MD) served as a positive control and PLA cells cultured in CM were a negative control.

### *Indirect immunofluorescence*

Control and induced PLA cells (5 weeks) were processed for IF on the basis of a previous study.<sup>31</sup> The antibodies used are outlined in Table 3: nuclei were visualized using 4',6-diamidino-2-phenylindole (DAPI) under a UV filter (VectaShield; Vector Laboratories, Burlingame, CA). Fluorescent and UV images were acquired with a SPOT-2 digital camera (Diagnostic Instruments, Sterling Heights, MI) and combined.

### *Western blot analysis*

To initially quantify changes in PLA collagen synthesis, Western blotting was performed as described elsewhere.<sup>30</sup> Briefly, control and osteo-induced PLA samples were resolved on 10% sodium dodecyl sulfate (SDS)–polyacrylamide gels (Bio-Rad, Hercules, CA) and transferred to polyvinylidene difluoride (PVDF) mem-

TABLE 1. COMPOSITION OF PROCESSED LIPOASPIRATE

Medium name	Medium	Serum	Supplementation
Control (CM)	DMEM	10% FBS	1% antibiotic–antimycotic
Osteogenic (OM)	DMEM	10% FBS	0.1 $\mu$ M dexamethasone, 50 $\mu$ M ascorbate 2-phosphate, 10 mM $\beta$ -glycerophosphate, 1% antibiotic–antimycotic <sup>a</sup>

<sup>a</sup>A 0.01  $\mu$ M concentration of 1,25-dihydroxyvitaminD<sub>3</sub> can be used in place of 0.01  $\mu$ M vitamin D.

**TABLE 2. OLIGONUCLEOTIDE PRIMER SEQUENCES AND EXPECTED PCR PRODUCT SIZES OF OSTEOGENIC GENES**

<i>Gene</i>	<i>Oligonucleotide primers</i>	<i>Product size (bp)</i>
Osteonectin (ON)	5'-TGTGGGAGCTAATCCTGTCC 3'-TCAGGACGTTCTTGAGCCAGT	400
Osteopontin (OP)	5'-GCTCTAGAATGAGAATTGCACTG 3'-GTCAATGGAGTCCTGGCTGT	270
Osteocalcin (OC)	5'-GCTCTAGAATGGCCCTCACACTC 3'-GCGATATCCTAGACCGGGCCGTAG	302
Core binding factor α-1 (CBFA-1)	5'-CTCACTACCACACCTACCTG 3'-TCAATAGGTCGCCAAACAGATTC	320
Collagen I (CNI) (α <sub>1</sub> chain)	5'-GAGAGAGAGGCTTCCCTGGT 3'-CACCACGATCACCCTCTTG	300
Alkaline phosphatase (AP)	5'-TGAAATATGCCCTGGAGC 3'-TCACGTTGTTCTGTTTAG 3'-CCCTCCACCAGAATCCAGTA	475

branes by conventional techniques. Membranes were probed for collagen I, III, IV, and V (Table 3) as described in a previous study.<sup>31</sup> Equivalent loading was confirmed by expression of α-actin (Santa Cruz Biotechnology, Santa Cruz, CA). Collagen expression levels were determined by densitometry and normalized to α-actin levels. Statistical comparisons were made by Student *t* test (paired) with significance at  $p \leq 0.05$ .

#### *TR-LIFS instrumentation, spectroscopic measurements, and data analysis*

To analyze the collagen composition of the osteogenic PLA samples, cells and matrices from each differentiation time point were harvested and investigated with a prototype TR-LIFS apparatus. The experimental setup used a fast digitizer and gated detection and was similar

to that previously described.<sup>12,13,27,28</sup> The light from a pulsed nitrogen laser (wavelength, 337.1 nm; repetition rate, 10 Hz) was focused onto the aperture of a fiber optic probe (UV-grade silica fiber; core diameter, 600 μm; NA, 0.22) and directed onto the sample from above (spot diameter, 1.5 mm; pulse width measured at the tip of the fiber, 3 ns full width at half maximum). The resulting fluorescence emission was collected by a fiber optic bundle (ring of 18 collection fibers of 200-μm core size), focused into a scanning monochromator, and detected by a gated multichannel plate photomultiplier tube (rise time, 0.3 ns) placed at the monochromator exit slit. The photomultiplier output was amplified (rise time, 0.35 ns; bandwidth, 1 GHz) and the entire fluorescent pulse from a single excitation laser pulse was recorded with a digital oscilloscope (bandwidth, 1 GHz; sampling frequency, 5 gigasamples/s).

**TABLE 3. ANTIBODIES USED AND SOURCES**

<i>Application</i>	<i>Collagen subtype</i>	<i>Antibody name</i>	<i>Clone</i>	<i>Source</i>
Immunofluorescence	I	(αCNI) MAb	COL-1	Sigma (St. Louis, MO)
	III	(αCNIII) MAb	NLI/42	Biogenesis (Kingston, NH)
	IV	(αCNIV) MAb	COL-94	Sigma (St. Louis, MO)
	V	(αCNV) MAb	NLI/64	Biogenesis (Kingston, NH)
			Anti-IgG-FITC	
Western blotting	I	(αCNI) goat PAb	C-18	Santa Cruz Biotechnology (Santa Cruz, CA)
	III	(αCNIII) goat PAb	C-15	Santa Cruz Biotechnology (Santa Cruz, CA)
	IV	(αCNIV) MAb	COL-94	Sigma (St. Louis, MO)
	V	(αCNV) MAb		Sigma (St. Louis, MO)
			Goat anti-mouse IgG-AP Donkey anti-goat IgG-AP	

The fluorescence emission of each sample was scanned in the 360- to 510-nm range at 5-nm intervals. The energy output of the laser was adjusted to 1  $\mu\text{J}/\text{pulse}$  (i.e., total energy delivered, <1.2  $\text{mJ}/\text{mm}^2$  per 250-s measurement). The time-integrated fluorescence (spectra emission) was computed from the measured fluorescence response pulses by integrating each pulse as a function of time for each wavelength. The constructed fluorescence spectra were corrected for background noise and normalized by dividing the fluorescence intensity at each emission wavelength by the peak fluorescence intensity. The time-resolved fluorescence (fluorescence decay) was analyzed by least-squares minimization of the weighted sum of the residuals.<sup>27</sup> A biexponential fit resulted in a trendless residual and a significant decrease in the residual sum of squares:

$$I_f(t) = a_1 e^{-t/\tau_1} + a_2 e^{-t/\tau_2}$$

The parameters  $\tau_1$  and  $\tau_2$  represent the fast and slow decay constants, respectively. The ratio  $A_1 = a_1/(a_1 + a_2)$  represents the fractional contribution of the fast-term component to the fluorescence impulse response function. Differences among sample means were assessed with a post hoc comparison test (Student–Newman–Keuls). All TR-LIFS data are reported as means  $\pm$  SE with the level of significance at  $p \leq 0.05$ .

In addition, spectroscopic measurements were recorded from five distinct collagen types: CNI from bovine Achilles tendon; CNI from calf skin; and CNIII, CNIV, and CNV from human placenta (Sigma, St. Louis, MO). Each sample (in powder dry form) was analyzed by TR-LIFS as described for PLA cells.

## RESULTS

### *Analysis of in vitro human bone formation, using PLA cells*

PLA cells have been identified in our laboratory and shown to have the potential to differentiate *in vitro* into the adipogenic, chondrogenic, osteogenic, and myogenic lineages.<sup>29–31</sup> Consistent with this work, PLA cells and NHOst positive controls cultured in osteogenic medium (OM) for up to 7 weeks produced a dense matrix that stained positively for alkaline phosphatase (AP) activity and matrix calcification in as few as 3 weeks of differentiation (Fig. 1A). Negligible staining for both AP activity and matrix calcium was observed in negative controls.

In addition, RT-PCR analysis confirmed the expression of multiple genes consistent with the osteogenic phenotype in induced PLA cells, including osteopontin (OP), osteonectin (ON), AP, and core-binding factor  $\alpha$ -1 (Cbfa-1) (Fig. 1B). The gene for the bone-specific marker osteocalcin was also detected in osteoinduced PLA cells. Taken together, the data indicate PLA osteogenic potential.

### *Detection of collagen expression: immunofluorescence and Western blot analysis*

PLA cells were analyzed for the expression of multiple collagens before TR-LIFS analysis. Nondifferentiated human PLA cells expressed CNI, CNIII, CNIV, and CNV. CNI was observed in both the cytoplasm and in extracellular fibrillar extensions (Fig. 2A). CNIII was confined to the perinuclear cytoplasm and no extracellu-

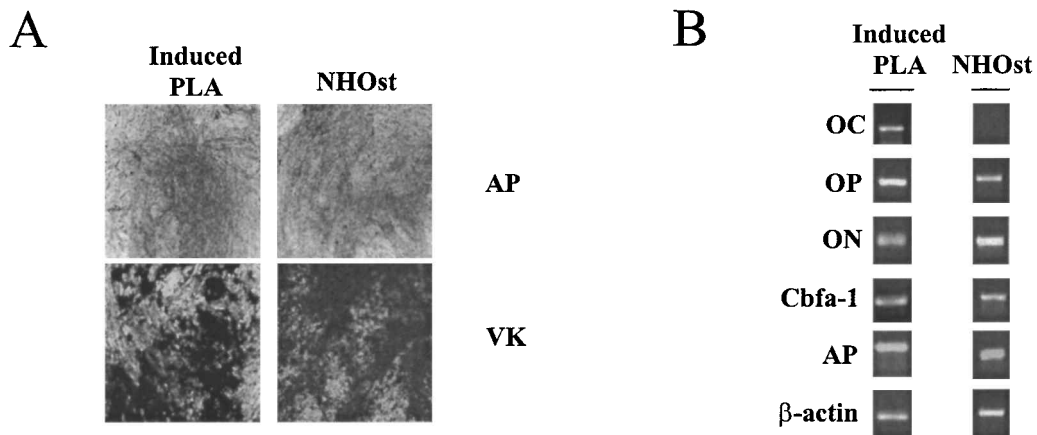


**FIG. 1.** PLA cells possess osteogenic capacity. (A) Human PLA cells induced with osteogenic medium (Induced PLA) for 3 weeks were stained for AP activity (AP, dark gray) and matrix mineralization (VK, black staining). A human osteoblast cell line (NHOst) served as a positive control. Original magnification,  $\times 200$ . (B) PLA cells cultured in OM for 3 weeks (Induced PLA) were analyzed by RT-PCR for the expression of osteocalcin (OC), osteopontin (OP), osteonectin (ON), core-binding factor 1 (Cbfa-1), and AP.

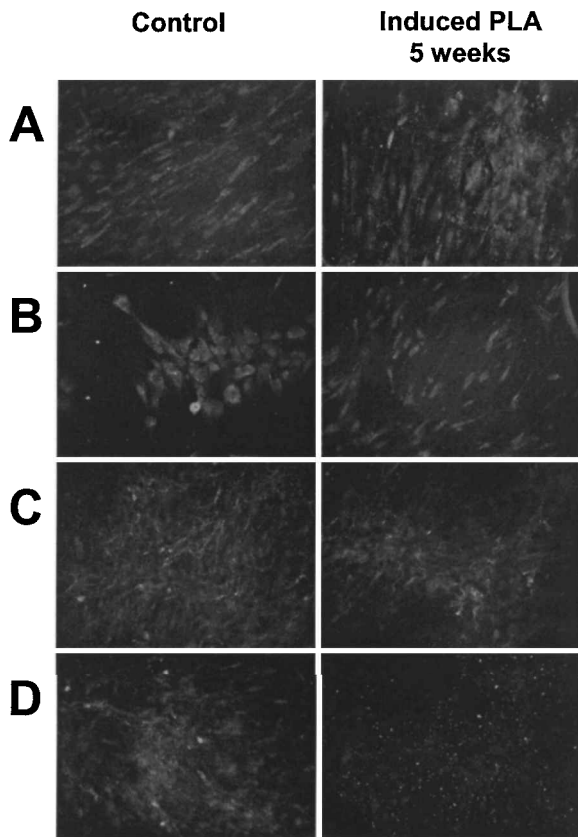


**FIG. 2.** PLA collagen expression: Immunofluorescence (IF) detection. PLA cells maintained in control medium (CM) and OM for 5 weeks were analyzed by IF for the expression of CN1 (A), CNIII (B), CNIV (C), and CNV (D). Samples were costained with DAPI to visualize nuclei (blue) and the images were combined. Original magnification,  $\times 400$ .

lar fiber formation was observed (Fig. 2B). Significant expression of CNIV and CNV was detected extracellularly, consistent with its role in the basement membrane, although a low level of intracellular CNIV expression was detected (Fig. 2C and D). Substantial collagen expression was detected after 5 weeks of osteogenic induction of PLA samples. Whereas both CN1 and CNIV expression patterns were unchanged, differences in CNIII and CNV patterns were noted. In contrast to noninduced cells, both intracellular and extracellular deposition of CNIII was observed in induced PLA samples. In addition, a decrease in CNV expression was observed in osteoinduced samples. Although IF analysis revealed collagen expression and localization, no significant difference in collagen expression levels could be discerned between the control and induced PLA samples, using this method.

To more quantitatively determine collagen expression on osteogenesis, PLA samples were analyzed by immunoblotting. The Western data correlated with the IF

data, confirming that both nondifferentiated and induced PLA cells synthesize CN1, CNIII, CNIV, and CNV (Fig. 3). Increased expression of all collagen types was measured in osteoinduced PLA samples after 3 weeks. Specifically, significant increases ( $p \leq 0.05$ ) in CN1 expression were restricted to between 3 and 5 weeks of differentiation, with no statistically significant change detected between the 5- and 7-week samples. Although a general trend for increased expression of CNIII, CNIV, and CNV was observed in osteoinduced PLA samples, the differences were not statistically significant.

#### Laser-induced fluorescence spectroscopy

Fluorescence emission spectra of nondifferentiated PLA cells, reconstructed by integration of the time-resolved decays along the time dimension, demonstrated broad emission with a peak at approximately 430 nm. The spectra of samples differentiated for 3, 5, and 7 weeks were similar to those of nondifferentiated samples, albeit with a slight red shift of the peak emission (Fig. 4A). These trends suggest that the fluorescence emission of both differentiated and control PLA sample originates from fluorophores with overlapping spectral emission.

Fluorescence emission was characterized by fast radiative lifetimes on the order of a few nanoseconds. For instance, the emission at 430 nm decayed to 5% of its maximum intensity in about 6 ns for nondifferentiated PLA samples and at a slightly slower rate (7 ns) for the 5- to 7-week osteogenic samples. The biexponential approximation of the fluorescence decay revealed that the decay constants ( $\tau_1$ ,  $\tau_2$ ,  $A_1$ ) varied with the number of weeks of differentiation and with emission wavelength

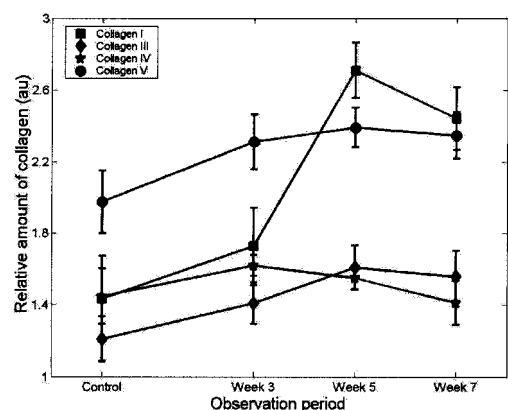


**FIG. 3.** PLA collagen expression: Western blot analysis. PLA cells maintained in CM and induced in OM for 3, 5, and 7 weeks were analyzed for CN1, CNIII, CNIV, and CNV expression by conventional immunoblotting. Collagen expression levels were determined by densitometry and normalized to  $\alpha$ -actin levels. Values were expressed as the relative amount of collagen expression (in arbitrary units, au) with respect to treatment time (observation period).

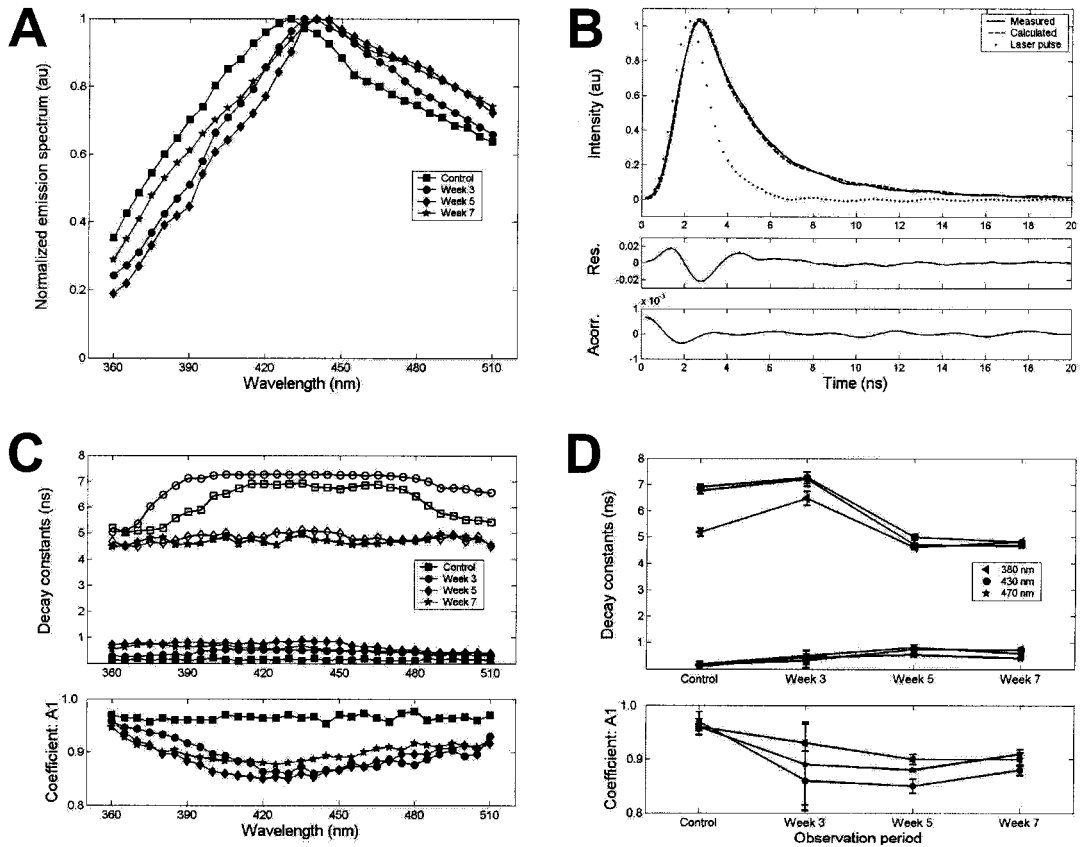


**FIG. 4.** Time-resolved laser-induced fluorescence spectroscopy analysis of PLA cells. Control and osteoinduced (3, 5, and 7 weeks) samples were analyzed by TR-LIFS. **(A)** Mean values for the fluorescence emission spectra measured ( $n = 3$ ). **(B)** Fluorescence emission response at 430 nm for week 7 (measured and reconstructed fluorescence pulses). Residuals and autocorrelation of the residuals (95% confidence interval). **(C)** Time-resolved decay constants along fluorescence emission spectra. *Top*: Fast-decay time constant (solid symbols), slow-decay time constants (open symbols). *Bottom*: Fractional contribution of the fast-decay time component  $A_1$ . Mean values for three patients. **(D)** Time-resolved decay constant—changes as a function of the period of differentiation at three wavelengths of emission (380 nm, blue-shifted range; 430 nm, peak emission range; 470 nm, red-shifted range). *Top*: Fast-decay time constant (solid symbols), slow-decay time constants (open symbols). *Bottom*: Fractional contribution of the fast-decay time component  $A_1$ . Values represent means  $\pm$  SE for the PLA samples obtained from three patients.

(Fig. 4C and D). The fast time decay constant at 430 nm ( $\tau_1$ ) increased on osteogenic differentiation (control samples,  $0.2 \pm 0.1$  ns; versus 5- and 7-week osteogenic samples,  $0.8 \pm 0.1$  ns). An opposite trend was exhibited by the slow time decay constant ( $\tau_2$ ), which decreased from about 7 to 5 ns after 5 weeks of osteoinduction. The fast-decay component,  $\tau_1$ , dominated the overall decay. The fractional contribution of the fast-decay component,  $A_1$ , was greater than 0.95 for the nondifferentiated PLA samples and approximately 0.8 for the 3-, 5-, and 7-week osteogenic samples. The decay constants for the nondifferentiated and 3-week PLA samples varied significantly with emission wavelength. In contrast, the decay constants for the 5- and 7-week samples were nearly constant along the emission spectra. The decay constant values retrieved from PLA samples measured at 3 weeks

showed significant variability between the three samples, whereas those retrieved from 5- and 7-week samples demonstrated similar characteristics among samples. Overall, the dynamics of the fluorescence decay of PLA samples varied with the time course of differentiation, from control to 7 weeks. However, the decay characteristics of 5- and 7-week osteogenic samples were similar, suggesting similar biochemical makeup for PLA cells differentiated for more than 3 weeks.

To confirm TR-LIFS analysis of the collagen composition of osteoinduced PLA samples, the fluorescence emission spectra of purified samples of CNI from calf skin, CNIII, CNIV, and CNIV (obtained commercially) were analyzed in the same fashion. Representative data are summarized in Table 4 and Fig. 5. A detailed description of the collagen time-resolved fluorescence data

**TABLE 4. FLUORESCENCE EMISSION SPECTRA OF COMMERCIAL COLLAGENS AND OSTEOGENIC PROCESSED LIPOASPIRATE SAMPLES**

Sample <sup>b</sup>	Peak emission (nm)	Time decay <sup>a</sup> $\tau_1$ (ns)	Time decay <sup>a</sup> $\tau_2$ (ns)	Coeff. <sup>a</sup> $A_1$
Type I (tendon)	380	$3.8 \pm 0.5$	$8.5 \pm 0.20$	$0.65 \pm 0.03$
Type I (calf skin)	420 (red shift)	<b><math>0.9 \pm 0.1</math></b>	<b><math>5.9 \pm 0.20</math></b>	<b><math>0.67 \pm 0.02</math></b>
Type III	390	$1.2 \pm 0.1$	$6.8 \pm 0.20$	$0.53 \pm 0.02$
Type IV	410	$0.7 \pm 0.1$	$5.7 \pm 0.15$	$0.67 \pm 0.01$
Type V	410	$0.7 \pm 0.1$	$5.8 \pm 0.15$	$0.77 \pm 0.01$
Noninduced PLA	430	$0.2 \pm 0.1$	$7.0 \pm 0.15$	$0.98 \pm 0.01$
Osteogenic PLA (5 to 7 week)	435–445 (red shift)	<b><math>0.8 \pm 0.1</math></b>	<b><math>5.0 \pm 0.15</math></b>	<b><math>0.88 \pm 0.02</math></b>

<sup>a</sup>Time decays and amplitude coefficients are given for each peak emission wavelength.

<sup>b</sup>Similarities are shown in boldface.

was previously reported by Marcu *et al.*<sup>28</sup> CNI from calf skin, and CNIV and CNV from placenta, all exhibited similar spectra and a short-lived fluorescence emission. The fast-decay component,  $\tau_1$ , was nearly constant ( $\sim 0.9$  ns) along the emission spectrum whereas the slow-decay component,  $\tau_2$ , increased slightly as a function of emission wavelength from 360 nm ( $\sim 4.5$  ns) to 510 nm ( $\sim 6$  ns). In contrast, a blue-shifted peak and a long-lived fluorescence emission characterized CNIII and CNI from bovine Achilles tendon (Table 4; and Ref. 28). For CNIII both fast- and slow-decay components were nearly constant along the emission spectrum ( $\tau_1$ ,  $\sim 1.2$  ns;  $\tau_2$ ,  $\sim 6.8$  ns), whereas for CNI the fluorescence decay characteristics are wavelength dependent (lower time decay values at wavelengths above 430 nm). In addition, the fluorescence emission of CNI was characterized by a narrow emission. The spectral emission characteristics of CNI

and CNIII investigated in the present study are in agreement with those described in early studies that used near-UV excitation wavelengths.<sup>5,10,27,32–34</sup> The distinct fluorescent signature (in both the spectral and time domains) observed between skin CNI and tendon CNI was likely a result of their different fluorescent cross-links.<sup>22,23,28</sup> Similarities in emission spectra were observed between the commercial CNI samples and the osteoinduced PLA samples, indicating the presence of CNI within the PLA matrix and confirming the IF and Western data. Interestingly, fluorescence emission spectra of the osteoinduced PLA samples resembled that of skin CNI rather than tendon CNI, suggesting a similar biochemical composition.

## DISCUSSION

In this study, we assessed the applicability of TR-LIFS to analyze nondestructively an osteogenic matrix produced by a novel population of stem cells. This is important because adipose-derived PLA cells may be a readily available source of stem cells, capable of being harvested in large quantities. As shown by Zuk *et al.*<sup>29,31</sup> and confirmed by Huang *et al.*<sup>35</sup> and Halvorsen *et al.*,<sup>36</sup> PLA cells possess multilineage potential, including osteogenic capacity. Specifically, PLA cells express significant levels of AP activity (a hallmark of preosteoblast matrix production by osteoblasts), undergo matrix calcification (a characteristic of the mature bone phenotype), and express multiple osteogenic genes and proteins.<sup>29,31,35</sup> Consistent with these previous studies, we confirm that osteoinduced PLA cells exhibit a time-dependent increase in AP activity and matrix mineralization and express several osteogenic genes, including osteonectin, osteopontin, osteocalcin,<sup>37,38</sup> and CBFA-1.<sup>39–41</sup> Moreover, using conventional methodologies for the analysis of collagen expression (IF and Western blotting) we demonstrate that both noninduced and differentiated PLA cells express CNI, CNIII, CNIV, and CNV

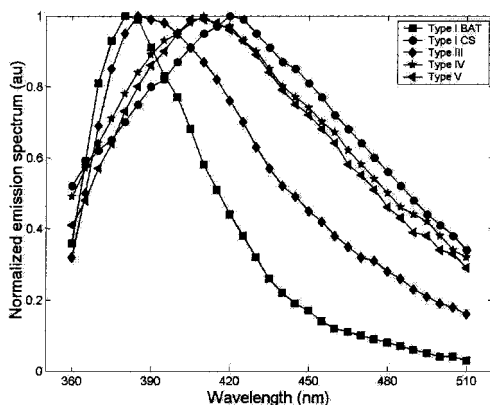


**FIG. 5.** Fluorescence emission spectra of commercial collagen types. Commercial samples of CNI from bovine Achilles tendon (BAT) and calf skin (CS), and placental collagens CNIII, CNIV, and CNV were analyzed by TR-LIFS as described for PLA samples.

collagens. However, only CNI exhibits a significant increase in synthesis over the 7 weeks of osteogenic differentiation. These results are consistent with studies of bone formation demonstrating that the basic building block of bone matrix is CNI, with trace amounts of CNIII and CNV present during certain stages of development.<sup>14,16,17,20</sup> The findings are also consistent with those of bone marrow mesenchymal stem cells (i.e., MSCs).<sup>42,43</sup> The capacity of MSCs to produce multiple ECM proteins together with various cytokines and cell surface integrins attests to a dynamic function in the marrow environment.<sup>44</sup> In this regard, PLA cells likely perform a similar multifactorial task in mature adipose tissue.

The fluorescence emission spectra of osteogenic PLA cells (Fig. 4A) are similar to those measured from purified skin CNI samples and from placental CNIV and CNV (broad fluorescence emission peaking at 420–430 nm). These data are supported by the Western data and suggest that the fluorescence emission of osteogenic PLA cells originates primarily from the CNI (skin-type cross-links), CNIV, and/or CNV collagen fluorescence signature. However, further analysis by TR-LIFS suggests that the fluorescent signature of osteoinduced PLA cells may be due primarily to the presence of CNI (Table 4 and Figs. 4 and 5).

Whereas the peak emission spectra of osteogenic PLA samples do not change significantly as a function of differentiation time, the fluorescence decay dynamics, as characterized by the time decay constants  $\tau_1$  and  $\tau_2$ , vary from nondifferentiated cells (week 0) to week 7 of differentiation, specifically changing after week 3. This trend is supported by the significant increase in collagen expression by PLA cells between 3 and 5 weeks of differentiation.

The fluorescence decay features of the 5- and 7-week osteogenic PLA samples resemble purified calf skin CNI and suggest that the time-resolved fluorescence data of PLA samples represent CNI overexpression after 3 weeks (Table 4; and Ref. 28). Although type IV and V collagens (with fast decay characteristics similar to type I skin collagen) are also likely to contribute to the overall fluorescence emission of the osteogenic PLA samples, they are unlikely to contribute to the change in fluorescence dynamics after 3 weeks. In support of this, no significant change in the amount of type IV and V collagen expression was observed during differentiation. It is essential to note that although both steady state and time-resolved fluorescence indicate CNI (calf skin), CNIV, and CNV as main contributors to overall fluorescence, only the time-resolved information allows monitoring of the relative expression of collagen over time. Moreover, the time domain information demonstrates that CNIII and tendon CNI molecules, possessing long-lived fluorescence, contribute minimally to PLA sample fluorescence.

It is noteworthy that because time-resolved information produced a clear distinction between CNI in skin and

in tendon, this study demonstrates that TR-LIFS is capable not only of detecting a significant increase in the synthesis and deposition of collagens within the ECM of osteoinduced PLA samples, but also of providing information regarding the nature of collagen cross-links. Collagen fluorescence on ultraviolet light excitation originates from several fluorescent chromophores including amino acids (e.g., tyrosine and phenylalanine) and cross-links (e.g., pyridinoline and pentosidine).<sup>21–28,45–47</sup> Collagens from various tissues are well known to exhibit age-related fluorescence at 380–460 nm (absorption spectra at 335–400 nm).<sup>26</sup> Thus the synthesis, posttranslational modification, or age-related changes of collagen cross-links would be reflected in the collagen fluorescence. These transformations play a critical role in collagen function in tissues. The ability of TR-LIFS to detect distinct collagen cross-links would supersede the information obtained by conventional methods and provide another advantage for its utilization. Further investigations are necessary to translate the fluorescence emission of specific collagen cross-links to distinct stages of osteogenic differentiation.

In summary, by evaluating the changes in the collagen expression within tissue sources, one can extract information regarding the status of tissue development. Our results demonstrate that TR-LIFS provides a nondestructive approach for monitoring the expression of distinct collagen types and the formation of collagen cross-links. Although the present work is focused on osteogenic differentiation and suggests TR-LIFS as a noninvasive analysis of tissue-engineered bone constructs, this study also represents a paradigm for the application of this technology to other tissue systems, such as type II collagen expression during chondrogenesis. As future research elucidates the temporal relationship of the diverse array of collagen to the functional status of mature bone and/or pathologic states, the potential ability of TR-LIFS to detect these alterations in a noninvasive, nonintrusive manner will provide an invaluable tool.

## ACKNOWLEDGMENTS

This work was funded in part by the Wunderman Family Foundation, the American Society for Aesthetic Plastic Surgery, the Plastic Surgery Educational Foundation, the Los Angeles Orthopedic Hospital Foundation, and National Institute of Health grants AR47637-01A1 (NIAMS), HL67377, and P41-RR01861 (Biomedical Simulations Resource, University of Southern California).

## REFERENCES

1. Tang, J., Zeng, F., Savage, H., Ho, P.P., and Afano, R.R. Fluorescence spectroscopic imaging to detect changes in

- collagen and elastin following laser tissue welding. *J. Clin. Laser Med. Surg.* **18**, 3, 2000.
2. Wagnieres, G.A., Star, W.M., and Wilson, B.C. In vivo fluorescence spectroscopy and imaging for oncological applications. *Photochem. Photobiol.* **68**, 603, 1998.
  3. Bigio, I.J., and Mourant, J.R. Ultraviolet and visible spectroscopies for tissue diagnostics: Fluorescence spectroscopy and elastic-scattering spectroscopy. *Phys. Med. Biol.* **42**, 803, 1997.
  4. Andersson-Engels, S., Klinteberg, C., Svanberg, K., and Svanberg, S. In-vivo fluorescence imaging for tissue diagnostics. *Phys. Med. Biol.* **42**, 815, 1997.
  5. Ramanujam, N., Mitchell, M.F., Mahadevan, A., Warren, S., Thomsen, S., Silva, E., and Richards-Kortum, E. In vivo diagnosis of cervical intraepithelial neoplasia using 337-nm-excited laser-induced fluorescence. *Proc. Natl. Acad. Sci. U.S.A.* **91**, 10193, 1994.
  6. Georgakoudi, I., Jacobson, B.C., Muller, M.G., Sheets, E.E., Badizadegan, K., Carr-Locke, D.L., Crum, C.P., Boone, C.W., Dasari, R.R., Van Dam, J., and Feld, M.S. NAD(P)H and collagen as in vivo quantitative fluorescent biomarkers of epithelial precancerous changes. *Cancer Res.* **62**, 682, 2002.
  7. Tang, G.C., Pradhan, A., and Alfano, R.R. Spectroscopic differences between human cancer and normal lung and breast tissues. *Lasers Surg. Med.* **9**, 290, 1989.
  8. Anastassopoulou, N., Arapoglou, B., Demakakos, P., Makropoulou, M.I., Paphiti, A., and Serafetinides, A.A. Spectroscopic characterization of carotid atherosclerotic plaque by laser induced fluorescence. *Lasers Surg. Med.* **28**, 67, 2001.
  9. Kinoshita, S., Seki, T., Fu Liu, T., and Kushida, T. Fluorescence of hematoporphyrin in living cells and in solution. *J. Photochem. Photobiol. B Biol.* **2**, 195, 1988.
  10. Sokolov, K., Galvan, J., Myakov, A., Lacy, A., Lotan, R., and Richards-Kortum, R. Realistic three-dimensional epithelial tissue phantoms for biomedical optics. *J. Biomed. Opt.* **7**, 148, 2002.
  11. Andersson-Engels, S., Johansson, J., Stenram, U., Svanberg, K., and Svanberg, S. Time-resolved laser-induced fluorescence spectroscopy for enhanced demarcation of human atherosclerotic plaques. *Photochem. Photobiol. B Biol.* **4**, 363, 1990.
  12. Maarek, J.M.I., Marcu, L., Fishbein, M.C., and Grundfest, W.S. Time-resolved fluorescence of human aortic wall: Use for improved identification of atherosclerotic lesions. *Lasers Surg. Med.* **27**, 241, 2000.
  13. Marcu, L., Fishbein, M.C., Maarek, J.M.I., and Grundfest, W.S. Discrimination of human coronary artery atherosclerotic lipid-rich lesions by time-resolved laser-induced fluorescence spectroscopy. *Arterioscler. Thromb. Vasc. Biol.* **21**, 1244, 2001.
  14. Lian, J.B., Stein, G.S., Canalis, E., Robey, P.G., and Boskey, A.L. In Favus, M.J., ed. *Primer on the Metabolic Bone Diseases and Disorders of Mineral Metabolism*. Philadelphia, PA: Lippincott Williams & Wilkins, 1999, pp. 14–27.
  15. Bland, Y.S., Critchlow, M.A., and Ashhurst, D.E. The expression of the fibrillar collagen genes during fracture healing: Heterogeneity of the matrices and differentiation of the osteoprogenitor cells. *J. Histochem.* **31**, 797, 1999.
  16. Collin, P., Nefussi, J.R., Wetterwald, A., Nicolas, V., Boy-Lefevre, M.L., Fleisch, H., and Forest, N. Expression of collagen, osteocalcin, and bone alkaline phosphatase in a mineralizing rat osteoblastic cell culture. *Calcif. Tissue Int.* **50**, 175, 1992.
  17. Poliard, A., Ronziere, M.C., Freyria, A.M., Lamblin, D., Herbage, D., and Kellerman, O. Lineage-dependent collagen expression and assembly during osteogenic or chondrogenic differentiation of a mesoblastic cell line. *Exp. Cell Res.* **253**, 385, 1999.
  18. Greenwald, J.A., Mehrara, B.J., Spector, J.A., Fagenholz, P.J., Saadeh, P.B., Steinbrech, D.S., Gittes, G.K., and Longaker, M.T. Immature versus mature dura mater. II. Differential expression of genes important to calvarial reossification. *Plast. Reconstr. Surg.* **106**, 630, 2000.
  19. Thalmeier, K., Meissner, P., Moosmann, S., Sagebiel, S., Wiest, I., and Huss, R. Mesenchymal differentiation and organ distribution of established human stromal cell lines in NOD/SCID mice. *Acta Haematol.* **105**, 159, 2001.
  20. Multimaki, P., Aro, H., and Vuorio, E. Differential expression of fibrillar collagen genes during callus formation. *Biochem. Biophys. Res. Commun.* **142**, 536, 1987.
  21. Uchiyama, A., Ohishi, T., Takahashi, M., Kushida, K., Inoue, T., Fujie, M., and Horiuchi, K. Fluorophores from aging human cartilage. *J. Biochem.* **110**, 714, 1991.
  22. Menter, J.M., Williamson, G.D., Carlyle, K., Moore, C.L., and Willis, I. Photochemistry of type I acid-soluble calf skin collagen: Dependence on excitation wavelength. *Photochem. Photobiol.* **62**, 402, 1995.
  23. Fujimoto, D. Isolation and characterization of a fluorescent material in bovine Achilles tendon collagen. *Biochem. Biophys. Res. Commun.* **76**, 1124, 1977.
  24. Sell, D.R., and Monnier, V.M. Structure elucidation of a senescence crosslink from human extracellular matrix. *J. Biol. Chem.* **264**, 21597, 1989.
  25. Theodossiou, T., Rapti, G.S., Hovhannisyann, V., Georgiou, E., Politopoulos, K., and Yova, D. Thermally induced irreversible conformational changes in collagen probed by optical second harmonic generation and laser-induced fluorescence. *Lasers Med. Sci.* **17**, 34, 2002.
  26. Fujimori, E. Changes induced by ozone and ultraviolet light in type I collagen: Bovine Achilles tendon collagen versus rat tail tendon collagen. *Eur. J. Biochem.* **152**, 299, 1985.
  27. Maarek, J.M.I., Marcu, L., Snyder, W.J., and Grundfest, W.S. Time-resolved fluorescence spectra of arterial fluorescent compounds: Reconstruction with the Laguerre expansion technique. *Photochem. Photobiol.* **71**, 178, 2000.
  28. Marcu, L., Cohen, D., Maarek, J.M.I., and Grundfest, W.S. Characterization of type I, II, III, IV, and V collagens by time-resolved laser-induced fluorescence spectroscopy. *SPIE* **3917**, 93, 2000.
  29. Zuk, P.A., Zhu, M., Mizuno, H., Huang, J.I., Futrell, J.W., Katz, A.J., Benhaim, P., Lorenz, H.P., and Hedrick, M.H. Multilineage cells from human adipose tissue: Implications for cell-based therapies. *Tissue Eng.* **7**, 211, 2001.
  30. Mizuno, H., Zuk, P.A., Zhu, M., Lorenz, H.P., Benhaim, P., and Hedrick, M.H. Myogenic differentiation of human processed lipoaspirate cells. *Plast. Reconstr. Surg.* **109**, 199, 2001.

31. Zuk, P.A., Zhu, M., Ashjian, P., DeUgarte, D.A., Huang, J.I., Mizuno, H., Alfonso, Z.C., Fraser, J.K., Benhaim, P., and Hedrick, M.H. Human adipose tissue is a source of multipotent stem cells. *Mol. Biol. Cell* **13**, 4279, 2002.
32. Laifer, L.I., O'Brien, K.M., Stetz, M.L., Gindi, G.R., Garland, T.J., and Deckelbaum, L.I. Biochemical basis for the difference between normal and atherosclerotic arterial fluorescence. *Circulation* **80**, 1893, 1989.
33. Andersson-Engels, S., Laert, R., Berg, M., D'Hallewin, M.A., Johansson, J., Stenram, U., Svanberg, K., and Svanberg, S. Fluorescence characteristics of atherosclerotic plaque and malignant tumors. *SPIE* **1426**, 31, 1991.
34. Papazoglou, T.G. Malignancies and atherosclerotic plaque diagnosis: Is laser induced fluorescence spectroscopy the ultimate solution? *J. Photochem. Photobiol. B Biol.* **28**, 3, 1995.
35. Huang, J.I., Beanes, S.R., Zhu, M., Lorenz, H.P., Hedrick, M.H., and Benhaim, P. Rat extramedullary adipose tissue as a source of osteochondrogenic progenitor cells. *Plast. Reconstr. Surg.* **109**, 1033, 2002.
36. Halvorsen, Y.D., Franklin, D., Bond, A.L., Hitt, D.C., Auchter, C., Boskey, A.L., Paschalis, E.P., Wilkison, W.O., and Gimble, J.M. Extracellular matrix mineralization and osteoblast gene expression by human adipose tissue-derived stromal cells. *Tissue Eng.* **7**, 729, 2001.
37. Owen, T.A., Aronow, M., Shalhoub, V., Barone, L.M., Wilming, L., Tassinari, M.S., Kennedy, M.B., Pockwinse, S., Lian, J.B., and Stein, G.S. Progressive development of the rat osteoblast phenotype in vitro: Reciprocal relationships in expression of genes associated with osteoblast proliferation and differentiation during formation of the bone extracellular matrix. *J. Cell. Physiol.* **143**, 420, 1990.
38. Malaval, L., Madrowski, D., Gupta, A.K., and Aubin, J.E. Cellular expression of bone-related proteins during in vitro osteogenesis in rat bone marrow stromal cell cultures. *J. Cell. Physiol.* **158**, 555, 1994.
39. Komori, T., Yagi, H., Nomura, S., Yamaguchi, A., Sasaki, K., Deguchi, K., Shimizu, Y., Bronson, R.T., Gao, Y.H., Inada, M., Sato, M., Okamoto, R., Kitamura, Y., Yoshiki, S., and Kishimoto, T. Targeted disruption of Cbfa1 results in complete lack of bone formation owing to maturational arrest of osteoblasts. *Cell* **89**, 755, 1997.
40. Otto, F., Thornell, A.P., Crompton, T., Denzel, A., Gilmour, K.C., Rosewell, I.R., Stamp, G.W., Bedington, R.S., Mundlos, S., Olsen, B.R., Selby, P.B., and Owen, M.J. Cbfa1, a candidate gene for cleidocranial dysplasia syndrome, is essential for osteoblast differentiation and bone development. *Cell* **89**, 765, 1997.
41. Banerjee, C., McCabe, L.R., Choi, J.Y., Hiebert, S.W., Stein, J.L., Stein, G.S., and Lian, J.B. Runt homology domain proteins in osteoblast differentiation: AML-3/CBFA1 is a major component of a bone specific complex. *J. Cell. Biochem.* **66**, 1, 1997.
42. Bentley, S.A., and Foidart, J. Some properties of marrow derived adherent cells in tissue culture. *Blood* **56**, 1006, 1980.
43. Zuckerman, K.S., and Wicha, M.S. Extracellular matrix production by adherent cells of long-term murine bone marrow cultures. *Blood* **61**, 540, 1983.
44. Conget, P.A., and Minguell, J.J. Phenotypical and functional properties of human bone marrow mesenchymal progenitor cells. *J. Cell. Physiol.* **181**, 67, 1999.
45. Garfield, R.E., Maul, H., Maner, W., Fittkow, C., Olson, G., Shi, L., and Saade, G.R. Uterine electromyography and light-induced fluorescence in the management of term and preterm labor. *J. Soc. Gyn. Invest.* **9**, 265, 2002.
46. Tian, W.D., Gillies, R., Brancalion, L., and Kollias, N. Aging and effects of ultraviolet A exposure may be quantified by fluorescence excitation spectroscopy in vivo. *J. Invest. Dermatol.* **16**, 840, 2001.
47. Muller, M.G., Valdez, T.A., Georgakoudi, I., Backman, V., Fuentes, C., Kabani, S., Laver, N., Wang, Z., Boone, C.W., Dasari, R.R., Shapshay, S.M., and Feld, M.S. Spectroscopic detection and evaluation of morphologic and biochemical changes in early human oral carcinoma. *Cancer* **97**, 1681, 2003.

Address reprint requests to:

*Laura Marcu, Ph.D.*

*Biophotonics Research and Technology*

*Development Laboratory*

*Department of Surgery, Cedars-Sinai Medical Center*

*8700 Beverly Blvd., Davis G149A*

*Los Angeles, CA 90048*

*E-mail: lmarcu@bmsrs.usc.edu*